

Modelling the impact of future changes in climate, CO₂ concentration and land use on natural ecosystems and the terrestrial carbon sink

P.E. Levy*, M.G.R. Cannell, A.D. Friend

Centre for Ecology and Hydrology, Bush Estate, Penicuik, Midlothian EH26 0QB, UK

Abstract

We used a global vegetation model, 'HyLand', to simulate the effects of changes in climate, CO₂ concentration and land use on natural ecosystems. Changes were prescribed by four SRES scenarios: A1f, A2, B1 and B2. Under all SRES scenarios simulated, the terrestrial biosphere is predicted to be a net sink for carbon over practically all of the 21st century. This sink peaks around 2050 and then diminishes rapidly towards the end of the century as a result of climate change. Averaged over the period 1990–2100, the net sink varies between scenarios, from ~2 to 6 Pg C yr⁻¹. Differences are largely the result of differences in CO₂ concentrations. Effects of climate change are substantially less, and counteract the effect of elevated CO₂. Land use change results in a loss of carbon to the atmosphere in the B2B scenario, in which the increase in cropland area continues. In the other scenarios, there is a decrease in croplands and grassland, with a corresponding increase in natural vegetation, resulting in a net sink to the biosphere. The credibility of these results depends on the accuracy of the predictions of land use change in the SRES scenarios, and these are highly uncertain.

As CO₂ is the dominating influence on the vegetation, the scenarios with high fossil fuel emissions, and thus the highest CO₂ concentrations (A1F & A2) generate the largest net terrestrial sink for carbon. This conclusion would change if these scenarios assumed continued deforestation and cropland expansion. Without the beneficial effects of elevated CO₂, the effects of climate change are much more severe. This is of concern, as the long-term and large-scale effects of elevated CO₂ are still open to question.

Differences between scenarios in the predicted global spatial pattern of net biome productivity and vegetation type are relatively small, and there are not major shifts in the dominant types. The regions predicted to be at greatest risk from global environmental change are Amazonia, the Sahel, South Central USA and Central Australia.

© 2003 Elsevier Ltd. All rights reserved.

1. Introduction

Global climate change will have impacts upon natural vegetation, affecting ecological and physiological processes, altering growing season length, biomass production, competition, and leading to shifts in species ranges and possible extinctions. As well as affecting climate, increases in the global atmospheric CO₂ concentration will affect natural vegetation directly. Many experiments have shown that increased CO₂ concentrations can increase photosynthesis and growth, and reduce stomatal conductance, though the response is variable between species and experimental conditions (Jarvis, 1998). The main human-induced factors changing vegetation in the recent past have been land use changes such as logging

for timber and clearance for agricultural use (Houghton, 1995). With the global population expected to nearly double over the next century, this is expected to continue to be a major influence.

Terrestrial ecosystems represent a large store of carbon, approximately three times that of the atmosphere. Changes in terrestrial ecosystems induced by any of the above causes are likely to result in changes in the amount of biomass and/or soil organic matter, and will result in a flux of carbon between the land and the atmosphere. Positive [or negative] feedback loops are possible if this carbon flux reinforces [or counteracts] the original change in the climate system (Cox et al., 2000).

Several models have been used to assess the impact of future climate change on global vegetation. These tend to be empirical in their treatment of plant physiology, e.g. several do not include CO₂ concentration as a variable in the calculation of primary production (Cramer et al., 1999). Very few incorporate land use

*Corresponding author. Tel.: +44-131-445-4343; fax: +44-131-445-3943.

E-mail address: plevy@ceh.ac.uk (P.E. Levy).

change, so model output represents potential vegetation, rather than the vegetation that is actually present (see McGuire et al., 2001; DeFries et al., 1999). Few studies have assessed the integrated effects of changes in climate, CO₂ concentration and land use on global vegetation over the next century. Here, we used the HyLand model to simulate the future impact of all of these global change factors, as prescribed by the IPCC Special Report on Emission Scenarios (SRES), on the functioning and distribution of ecosystems.

Specifically, we aimed to:

- (i) Quantify the carbon source/sink strength of the terrestrial biosphere.
- (ii) Quantify the contribution of the various factors to the net carbon flux.
- (iii) Predict the future global distribution of vegetation types.
- (iv) Identify regions under greatest threat from global change.

2. Methods

2.1. Model

A dynamic global vegetation model (Hybrid) was developed previously to predict the impact of future climates on global vegetation (Friend et al., 1997; Friend and White, 2000). The model is process-based and is able to simulate transient changes in the growth and distribution of different biomes year by year. A further version of the model (HyLand) was constructed to simulate the transient effects of changes in land use on vegetation properties and carbon stocks. Changes to the model of Friend et al. (1997) are described in Table 1 and Appendix A.

2.2. SRES scenarios

The future emissions of greenhouse gases will depend on future trends in the global economy, population growth, and technological change. The recognition that these factors are linked led the IPCC to develop a set of scenarios, in which change in each factor is consistent with a particular ‘storyline’, published as the SRES (IPCC, 2000). Four storylines were defined to encompass a range of possible ways in which socio-economics may develop over the next century. The storylines are differentiated in two main dimensions: the balance between economic and environmental concerns, and the heterogeneity of regional development patterns. The four storylines can be briefly characterised as follows (see Arnell et al., 2004).

The A1 scenario envisages very rapid economic growth with increasing globalisation, an increase in general wealth, with convergence between regions and reduced differences in regional per capita income. Materialist–consumerist values predominant, with rapid technological change and low population growth. Three variants within this family make different assumptions about sources of energy for this rapid growth: fossil intensive (A1F), non-fossil fuels (A1T) or a balance across all sources (A1B).

The A2 scenario is a heterogeneous, market-led world, with less rapid population and economic growth than A1. The underlying theme is self-reliance and preservation of local identities. Economic growth is regionally orientated, and hence both income growth and technological change are regionally diverse. Fertility patterns across regions converge slowly, resulting in high population growth.

The B1 scenario has the same low population growth as A1, but development takes a much more environmentally sustainable pathway, with global-scale

Table 1
Processes represented in HyLand, the approach taken and the principal source describing it

Process	Approach	Source
Competition	Simple, empirical ^a	This paper
Photosynthesis	Leaf: biochemistry Canopy: optimisation	Farquhar and von Caemmerer (1982) Sellers et al. (1992)
Plant respiration	Fixed fraction of gross photosynthesis ^a	Waring et al. (1998)
Stomatal conductance	Empirical	Jarvis (1976), and Stewart (1988)
Transpiration	Energy balance/Penman-monteith equation	Friend (1995), and Monteith and Unsworth (1990)
Nitrogen uptake	Prescribed concentrations ^a	
Phenology	Not represented ^a	
Litter production	Fixed turnover rates	Friend et al. (1997); this paper
Allocation	Fixed coefficients ^a	This paper
Tree mass/height	Not represented ^a	
Decomposition	Adapted century model	Comins and McMurtrie (1993)
Hydrology	Single layer bucket	Friend et al. (1997)
Land use change	Prescribed effects of clear-felling and cropping ^a	This paper

^aDenotes differences from Friend et al. (1997).

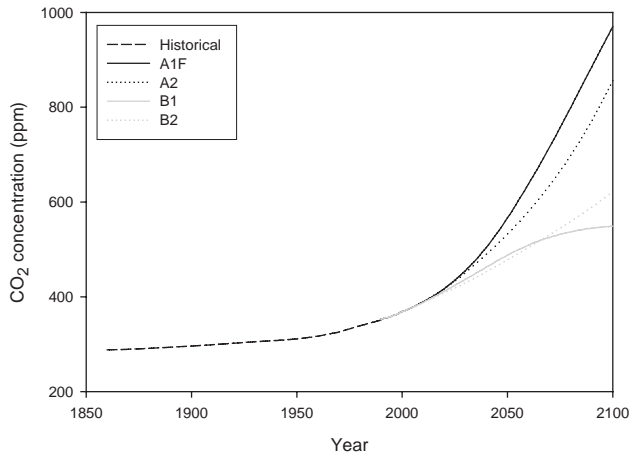


Fig. 1. CO₂ concentration from historical sources and the four SRES scenarios.

cooperation and regulation. Clean and efficient technologies are introduced. The emphasis is on global solutions to achieving economic, social and environmental sustainability.

In the B2 scenario, population increases at a lower rate than A2, with development following environmentally, economically and socially sustainable, locally orientated pathways.

The SRES scenarios divide the globe up into four regions which are considered to be homogeneous socio-economically: OECD countries (Europe, North America & Australia); former states of the Soviet Union; Asia; and Africa & Latin America.

2.3. CO₂ concentration data

The conversions between time courses of CO₂ emissions and CO₂ concentration for each of the four SRES scenarios were obtained from the ISAM model (IPCC, 2001). The highest CO₂ concentration is achieved in the A1F scenario, reaching 970 ppm by 2100 (Fig. 1). The B1 scenario has the lowest CO₂ concentration, reaching 549 ppm in 2100. The A2 and B2 scenarios are intermediate.

2.4. Climate data

Greenhouse gas emissions from the four SRES scenarios were used as inputs to HadCM3, the most recent version of the Hadley Centre global climate model. Compared with earlier versions, the model includes improved representations of some key processes, such as the influence of sulphate aerosols, and does not require a flux correction to maintain a stable climate. HadCM3 uses a 96×73 global grid (3.75° longitude \times 2.5° latitude).

One simulation was performed with HadCM3 for each of the A1F and B1 scenarios. For the A2 scenario,

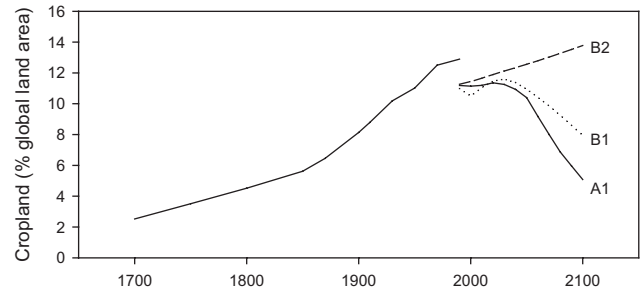


Fig. 2. Global cropland area from historical sources (Ramankutty and Foley, 1999) and SRES land use change scenarios.

three ensemble simulations with the same forcing but different initial boundary conditions were performed, to obtain a measure of the natural climatic variability. Similarly, two ensemble simulations were performed for the B2 scenarios. Because of the computation time of the HyLand model only one of these simulations was used for each scenario, referred to as A2c and B2b. The HadCM3 outputs were used as off-line inputs to the HyLand model, i.e. the models were not run interactively.

The global pattern of change in temperature and precipitation is similar in the seven scenarios, with the temperature increase greatest at high latitude. Precipitation also increases at high latitudes and across much of Asia. Precipitation decreases in Southern Africa, in the Mediterranean, and in much of Latin America.

2.5. Land use data

Data on the historical expansion of cropland have recently been published (Ramankutty and Foley, 1999). These data cover the period 1700–1992 at approximately 30-year resolution, and encompass the global land surface at 0.5 degree spatial resolution. These data were averaged up to the 3.75×2.5 degree used by HadCM3 to prescribe the historical course of land use change in the HyLand model. The data shows an increase in cropland from around 2% of the global land area in 1700, to over 13% in 1990 (Fig. 2).

The SRES A1F, B1 and B2 scenarios include land use data for the following categories: cropland, forest, grassland, and ‘other’. No land use data exist for the A2 scenario, so the A1F data were used instead. These data are available for the four SRES regions at decadal intervals between 1990 and 2100 (Fig. 2). As no data with higher spatial resolution were available, the SRES regional data were used to derive trends in land use relative to 1990, which were applied to all cells within that region. In this way, the appropriate temporal change is represented whilst maintaining the more complex spatial pattern at 3.75×2.5 degrees present in 1990. This also means that the discontinuity between the historical and SRES data in Fig. 2 does not influence the

model. Fig. 2 shows that the area of cropland is predicted to decline markedly in the A1 and B1 scenarios (after an initial rise in B1 until 2030). Only in the B2 scenario is the area of cropland predicted to increase.

At each point on the 3.75×2.5 degree grid, ten plots were represented, each with a discrete land use type. As the fraction of cropland increased over time, the appropriate number of plots were switched from the natural vegetation type, via the clear-felled state, to the cropland type. The effect of land use type on the modelled vegetation are described in Appendix A. Where the fraction of cropland decreased over time, the appropriate number of plots were switched from the cropland type to the natural vegetation type. Thus both cropland expansion and abandonment can be represented in the model.

2.6. Simulations

Details of the simulations performed are summarised in Table 2. The HyLand model was run for a period of 400 years with pre-industrial conditions specified as inputs: a CO₂ concentration of 288 ppm, the HadCM3 climate for the decade 1860–1869, and the land use as prescribed by Ramankutty and Foley (1999) for 1700. During this period, the model state variables reached equilibrium, and all values were saved at the end of this spin-up period. Using these saved values for initialisation, the model was then run for a 290-year historical period, from 1700 to 1990, using the historical CO₂ data from ISAM, the Ramankutty and Foley (1999) data for land use change and the HadCM3 climate data for 1860 onwards. Again, all values were saved at the end of the run and used as the initial values for the SRES scenario runs.

Four simulations were run, corresponding to the A1F, A2c, B1 and B2b scenarios. These covered the period

1990–2100 and used the SRES data for CO₂, land use change and the HadCM3 climate data. In a further set of simulations for each SRES scenario, one set of these inputs to the model was held constant at the 1990 level over the period 1990–2100. Thus for each scenario, there were three further simulations in which either: the CO₂ concentration was held at 353 ppm; the 1990s climate was used; or the 1990 land use pattern was retained. This allowed the separation of the effects of climate change, elevated CO₂ and land use change. There thus 16 simulations in total for the period 1990–2100.

3. Results

Fig. 3 shows the global fluxes of carbon predicted by HyLand between 1700 and 2100. The vegetation is initially in equilibrium with the pre-industrial climate, so net ecosystem productivity (NEP, i.e. net primary productivity minus heterotrophic respiration) is near zero before 1850. The flux resulting directly from land use change (i.e. fire and log-removal, hereafter referred to as the land use change flux, LUCF) is small during this period, producing a small, negative net biome productivity (NBP, equal to NEP plus LUCF). Fluxes from the atmosphere to the land (sinks) are considered to be positive.

Between 1850 and the present day, NEP gradually becomes more positive, reaching 2.6 Pg C yr^{-1} in the 1990s. LUCF also increases markedly from around 1850 to the present day, and for most of this period, exceeds NEP, resulting in NBP remaining negative until the 1970s. Though somewhat higher, the model predictions for NBP in the 1980s and 1990s are close to the most recent estimates based on inverse modelling of trends in atmospheric CO₂ and O₂ concentrations (IPCC, 2001). Similarly, the model predictions of LUCF are within the limits of uncertainty on inventory or book-keeping-

Table 2
Scenarios for climate, CO₂ (ppm) and land use (LU) used in four global-scale simulations

Simulation	'Spin-up' conditions			1700–1989			1990–2100		
	Climate	CO ₂	LU	Climate	CO ₂	LU	Climate	CO ₂	LU
A1F	Pre-industrial (HadCM3 1860–1869)	288	Pre-industrial ^a	HadCM3 simulation (from 1860 onwards)	288–352	Ramankutty and Foley (1999)	A1F–HadCM3	353–970	A1F
A2							A2c–HadCM3	353–856	A1F
B1							B1–HadCM3	353–549	B1
B2							B2b–HadCM3	353–621	B2

A1F, A2, B1 and B2 are IPCC SRES scenarios. HadCM3 is the UK Hadley Climate Model.

^aBased on the data of Ramankutty and Foley (1999) for 1700.

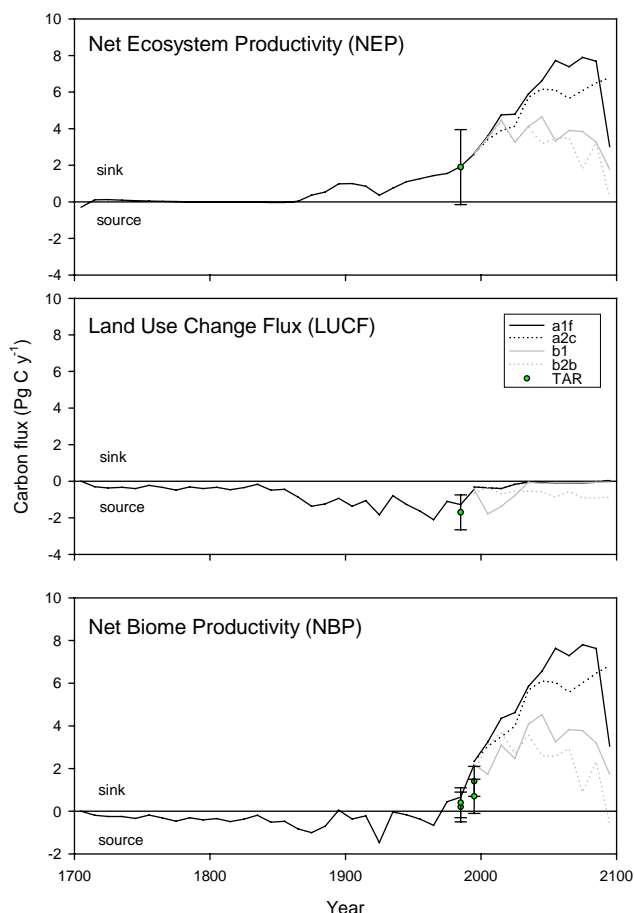


Fig. 3. Global fluxes of carbon predicted using the SRES A1F, A2c, B1 & B2b scenarios for climate and CO₂. Fluxes shown are net ecosystem productivity (NEP, net primary productivity minus heterotrophic respiration), the flux resulting directly from land use change (LUCF), and net biome productivity (NBP, NEP plus LUCF). Fluxes from the atmosphere to the land (sinks) are denoted positive throughout. Also shown are independent values based on inverse modelling of trends in atmospheric CO₂ and O₂ concentrations from the Third Assessment Report of the IPCC (TAR).

based estimates (also from IPCC, 2001). The residual of the inverse modelling-based NBP and the inventory-based LUCF values gives the best available estimates of NEP based (indirectly) on observations. The almost exact correspondence with the model prediction of NEP in the 1980s is probably spurious, as the uncertainty in the observation is so large.

After 1990, there is a continuing rise in NEP following the rise in CO₂ concentration and temperature. This lasts until around the middle of the century in most scenarios, then begins to decline, to near zero in the B2 scenario. The exception is the A2 scenario, where NEP continues to rise over the whole century, though more slowly in the latter half. In the A1F scenario, LUCF returns to near zero after 1990, as the scenario predicts little further conversion of natural vegetation to cropland. In the B1 scenario, there is an initial peak in

LUCF in the early part of the 21st century, whereafter it returns to near zero, as in the A1F scenario. In both these scenarios, the decline in cropland area (Fig. 2) contributes strongly to the high NEP, as abandoned cropland is converted back to the natural state where regrowth of woody vegetation is permitted. Note that this flux arises from land use change indirectly, so is accounted for as NEP not LUCF under the definitions given above. NBP results from the net effect of NEP and LUCF, and as LUCF is generally small, it largely follows the pattern in NEP. The terrestrial vegetation thus acts as a net sink over the 21st century in all scenarios, with the peak values ranging from 4 to 8 Pg C yr⁻¹ in the different scenarios.

Fig. 4 shows the effects of climate change, elevated CO₂ and land use change on the simulated NBP over the period 1990–2100. These are calculated as the difference between NBP in the standard SRES scenario and that when the given input is held constant. In all scenarios, elevated CO₂ has the largest influence on NBP, and this effect is greatest in the A1F and A2C scenarios, where CO₂ concentrations reach the highest values. The effect of climate change is considerably smaller, and acts to reduce NBP in all scenarios. The influence of land use change is of a similar magnitude, but may be positive or negative, depending on the scenario (note that here, both direct and indirect effects of land use change are included in this measure). The B2B scenario is the only one in which croplands increase, resulting in a net source from deforestation. In the other scenarios, cropland is abandoned, and natural vegetation permitted to increase, resulting in a net sink to forest regrowth.

Fig. 5 shows the global distribution of total ecosystem carbon (plant plus soil) predicted by the model for 2100.

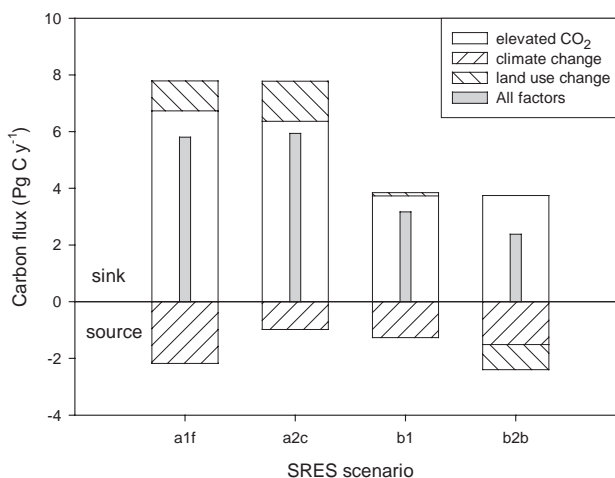


Fig. 4. Influence of the three main input factors on the predicted NBP over the period 1990–2100 in four SRES scenarios (A1F, A2C, B1 & B2B). Grey bars show the predicted value when all factors are included in the simulation; other bars show the contribution from climate change, elevated CO₂ and land use change to this value. Note that there are interaction effects.

The spatial pattern in all scenarios is roughly similar, and broadly follows the current distribution of vegetation biomass. Agreement between model predictions for the current day and the independent data of Olson et al. (1983) suggest we can have a degree of confidence in the model (Levy et al., in preparation). Differences between the scenarios are more apparent if the change in ecosystem carbon over the simulation is plotted rather than the total (Fig. 6). This shows that most regions are predicted to be carbon sinks, with the exceptions of Amazonia, the Sahel, Central Australia, Central USA

(not in A2), and some areas of Eastern Europe, Russia and China (B2 only). The strong source from the Amazonian region is a consistent feature in all scenarios.

Fig. 7 shows the geographical distribution of the effects of climate change, elevated CO_2 and land use change on the simulated NBP in the B2 scenario. This shows that the predicted loss of carbon in Amazonia, the Sahel and Central Australia is related to climate change, as these sources are not seen when climate is held constant (Fig. 7b). When CO_2 is held constant, large areas of the globe become net sources of carbon,

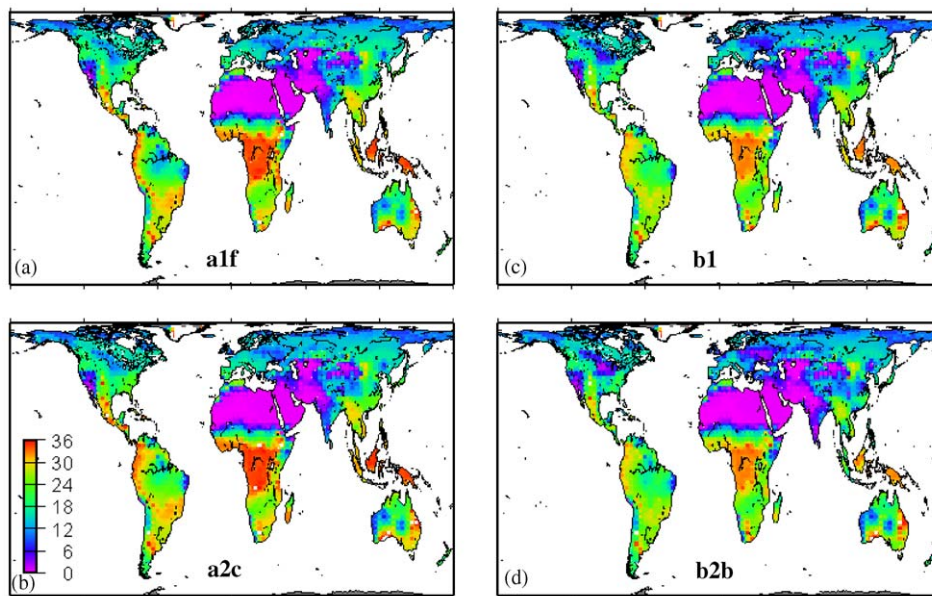


Fig. 5. Predicted total carbon (plant + soil, kg C m^{-2}) in 2100 in the four SRES scenarios.

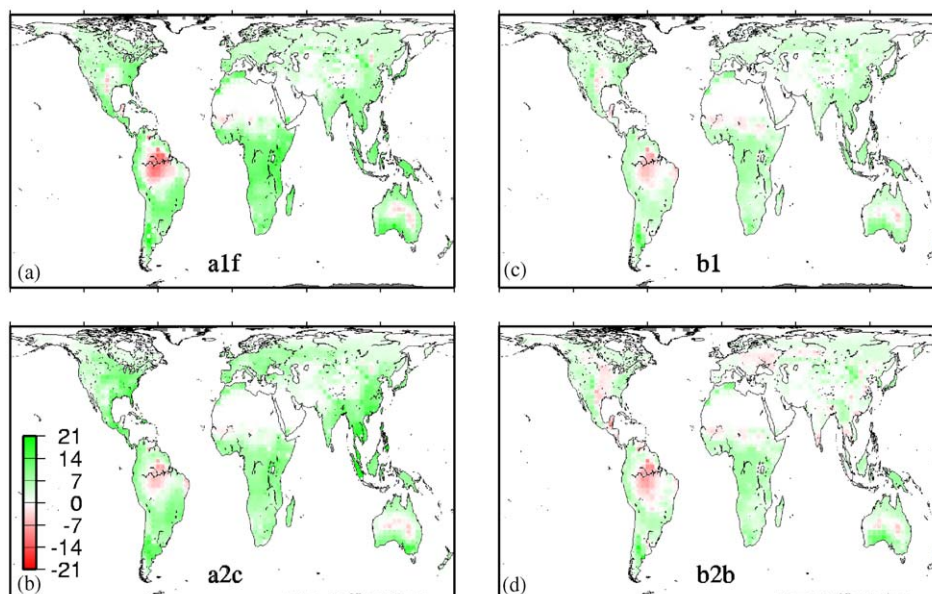


Fig. 6. Predicted change in total carbon (plant + soil, kg C m^{-2}) between 1990 and 2100 in the four SRES scenarios.

including the African rainforest and large parts of the South American forest and S.E. Asia (Fig. 7c). The relatively small predicted source regions in Central Asia, China and India are related to land use change, as these sources are not seen in Fig. 7d.

Fig. 8 shows the predicted change in total ecosystem carbon in the four SRES scenarios, classified by vegetation type. The biggest carbon gains are found in

the broad-leaved forest class, and this has the highest median value in all scenarios, though the largest losses are also found in this class. Grasslands and needle-leaved forest rank second or third depending on the scenario. Needle-leaved forest show notably smaller variation. The spatial distribution of vegetation types varies little between scenarios, largely because the spatial patterns in the input variables specified by the

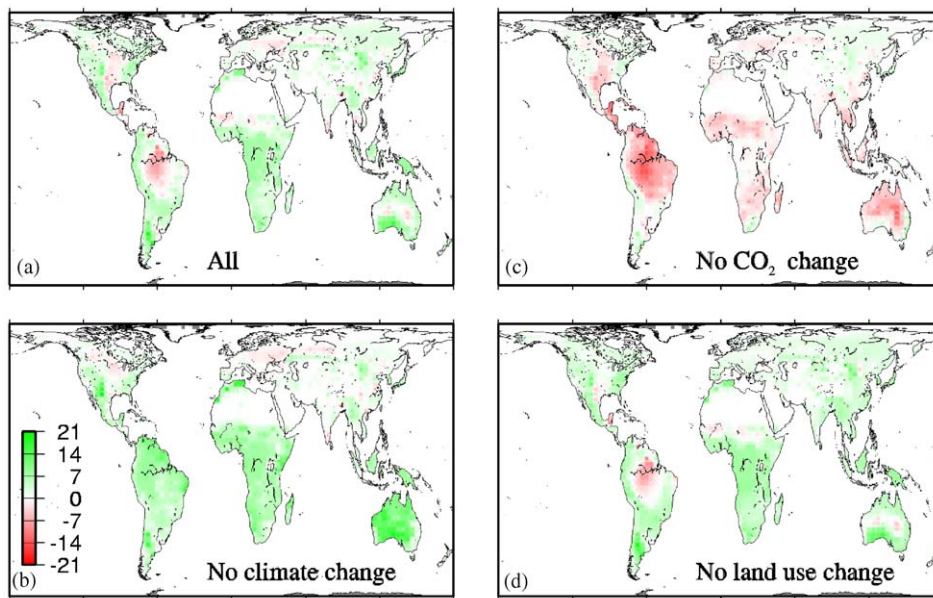


Fig. 7. Predicted change in total carbon (plant + soil, kg C m^{-2}) between 1990 and 2100 in the B2b SRES scenario where one set of these inputs to the model was held constant at the 1990 level. In addition to the standard scenario (a), there were three further simulations in which either: the 1990s climate was used (b); the CO_2 concentration was held at 353 ppm (c); or the 1990 land use pattern was retained (d).

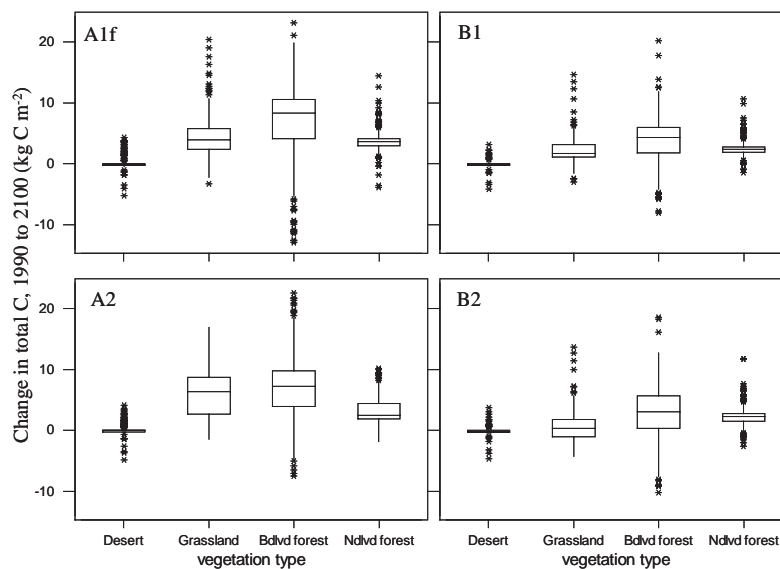


Fig. 8. Boxplots showing the distribution of the losses and gains of total carbon (plant + soil, kg C m^{-2}) between 1990 and 2100 in the four SRES scenarios, classified by vegetation type. Boxes show the interquartile range with the horizontal line indicating the median. The vertical lines extend from the box to the lowest and highest observations that are still inside the region defined by the following limits: $Q1 - 1.5(Q3 - Q1)$ or $Q3 + 1.5(Q3 - Q1)$, where $Q1$ and $Q3$ are the first and third quartiles. Outlying points outside of these limits are plotted as asterisks.

four SRES scenarios are generally similar. The dominant type of vegetation at any particular location is therefore generally the same in the different scenarios, irrespective of carbon gains or losses.

4. Discussion

The terrestrial biosphere is predicted to be a net sink for carbon during the 21st century in all four SRES scenarios simulated. As CO₂ is the dominating influence on the vegetation (enhancing net primary productivity) the scenarios with high fossil fuel emissions, and thus the highest CO₂ concentrations (A1F & A2) have the largest net sink for carbon. This would change if these scenarios also assumed continued deforestation and cropland expansion. The spatial pattern in vegetation losses and gains is broadly similar in all scenarios, with losses consistently being seen in Amazonia, the Sahel, South Central USA and Central Australia. These are the regions predicted to be at greatest risk from the deleterious effects of the simulated global environmental change. The spatial distribution of vegetation types is very similar in all scenarios, and there are not major shifts in the dominant types. Without the beneficial effects of elevated CO₂, the effects of climate change (warming and drought) are much more severe. This is of some serious concern, as the long-term and large-scale effects of elevated CO₂ are still open to question.

Under all SRES scenarios simulated, the terrestrial biosphere is predicted to be a net sink for carbon over practically all of the 21st century. This sink peaks around 2050 and then diminishes rapidly towards the end of the century as a result of climate change. Averaged over the period 1990–2100, the net sink varies between scenarios, from ~2 to 6 Pg C yr⁻¹. This sink is the balance between the effects of CO₂, climate and land use change. Of these, CO₂ is the dominant influence producing the net sink. The effect of climate change can be positive or negative, depending on the location, but on balance has a negative effect. This largely results from the decline in the Amazonian forest areas where rainfall declines markedly. The reduction in rainfall in the Amazon basin is not reproduced in all GCMs, so there is considerable uncertainty in this result.

The effect of land use change can also be positive or negative, depending on whether cropland is contracting or expanding in the scenario (i.e. whether natural vegetation is regrowing or being deforested). Here, cropland contracts in two out of the three land use scenarios. This may seem to be a rather optimistic view of future world development, in that global forest area does not decline overall, despite expected continued tropical deforestation, and cropland areas do not generally expand despite continued population growth. There is large uncertainty in the future trend in cropland

area as population increases, as illustrated in Fig. 9. Until very recently, cropland area has shown a linear increase with population. However, in the last 50 years, in which the population has doubled, the increase in cropland area has been very small. How this trend will continue with a possible further doubling of the population over the next century is clearly highly uncertain. The three SRES scenarios in Fig. 9 cover the possibilities of a slight increase in cropland (B2), and of a substantial decrease (A1F and B1). We suggest that the possibility of substantial increase should also be included. Recent studies have estimated that, based on soil, water and climatic constraints, the area of cropland could still be increased by an additional 120% of the current value, i.e. to nearly 30% of the land area (Bot et al., 2000; Ramankutty et al., 2002). This expansion would necessarily result in substantial deforestation. Deforestation of areas for permanent pasture rather than cropland may be a significant term, particularly in South America. However, this land use change is not included in these simulations as (i) the SRES land use data do not distinguish natural grassland from that which is artificially created, and (ii) there are no data available on the historical expansion of pasture land.

Appendix A. Model description

The Hybrid model, fully described elsewhere (Friend et al., 1997; Friend and White, 2000) was simplified, taking a more top-down approach, removing the individual-tree simulation in the original ‘gap’ model, retaining all the vegetation and soil compartments, but with simplified hydrology and N dynamics. The model uses a daily time-step. Inputs were climate variables, atmospheric CO₂ concentration, and land use change. Here we describe the major differences from Friend et al. (1997) and note where the changes described in Friend and White (2000) are included.

A.1. Vegetation

- Three (cf. eight) plant types were represented: herbs, broad-leaved and need-leaved trees. Individual trees were not represented. The vertical dimension in the canopy was ignored, except that the herbaceous layer was implicitly beneath the tree canopy.
- Plant respiration (i.e. respiration not accounted for in net daytime photosynthesis) was assumed to be half of gross photosynthesis. Several recent studies have indicated that this assumption may be a good approximation of reality (Gifford, 1995; Waring et al., 1998; Dewar et al., 1999; Thornley and Cannell, 2000), better than the assumption that maintenance respiration is a linear function of the total carbon content of each of the plant compartments

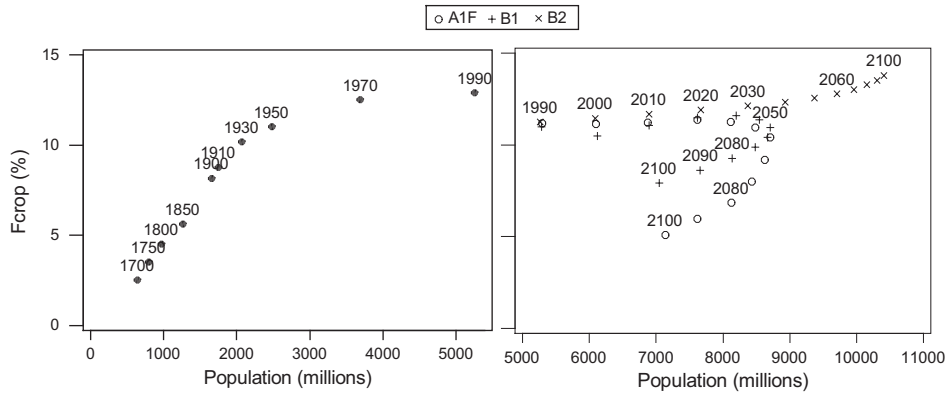


Fig. 9. Relationship between global population and the area of cropland as a fraction of the global land area (F_{crop} , %), from historical sources (left-hand panel) and SRES scenarios (right-hand panel).

and an exponential function of air temperature (Ryan, 1991).

- Nitrogen dynamics were not simulated, but the nitrogen content of the top layer of foliage (N_{top}) was prescribed as 1.3 kg N m^{-2} .
- NPP was allocated in fixed ratios to foliage (0.1 for trees, 0.28 for herbs) structure (0.7 for trees, 0.33 for herbs) and roots (0.2 for trees, 0.39 for herbs).
- Leaf area index was the product of foliage carbon and specific leaf area ($36 \text{ m}^2 \text{ kg C}^{-1}$ for herbs and broad-leaved trees, $18 \text{ m}^2 \text{ kg C}^{-1}$ for needle-leaved trees).
- Litter fall was calculated from fixed turnover rates for foliage (0.8, 1 and 6 years for herbs, broad-leaved and needle-leaved trees, respectively) structure (0.8, 20, 10 years for herbs, broad-leaved and needle-leaved trees, respectively) and roots (0.5 years for all types).
- If the stem carbon of one tree type was within $\pm 50\%$ of that of the other, then PAR was shared equally; if not the lesser type was excluded. Herbs dominated if the woody canopy was sparse. PAR at the top of the canopy was scaled to ensure that the sum of light used did not exceed that available. All plant types were initialised at 0.1 kg C m^{-2} allocated between structural compartments with the same fractions as for NPP (see above).

A.2. Soil

- Soil water capacity was calculated as a linear function of soil carbon (Friend and White, 2000). When the soil contained 10% more than its capacity there was drainage. Soil water-filled space was calculated from soil water content and a prescribed soil texture as described by Friend and White (2000). Soil water potential was calculated from soil water content.
- In order to deal effectively with deforestation, pools of coarse surface and below-ground structural litter

were added to the decomposition sub-model of Friend et al. (1997) with residence times of 73 and 53 years, respectively, when soil temperature and moisture factors were unity. These long residence times delayed carbon loss after clearfelling (see below).

- Since soil carbon may take centuries to reach equilibrium, the pool size was initialised in the 'spin-up' run with an estimated soil carbon content derived from the observed relationship between soil carbon and pre-industrial precipitation and temperature (Friend and White, 2000).

A.3. Land use

Three land use options were employed, which were assumed to alter carbon pools and fluxes as follows:

- *Natural vegetation*: No constraints placed upon the simulated vegetation.
- *Deforestation (clearfelled forest)*: (i) It was assumed that 64% of the above-ground stem carbon was removed instantly by fire or as logs. No account was taken of the fate of forest products. Houghton (1991) assumed that 33% of the original vegetation was left to decay on site at the time of clearing; thus 67% was lost to burning or removal. If 30% of stem mass is stump and below-ground and all fine plus 30% of coarse above-ground litter is burned (Hao et al., 1990), then about 64% of above-ground stem must be removed to leave 33% of the original carbon on site (70% of stem is assumed to be coarse). (ii) Clear-cutting was immediately followed by a fire, which oxidized 30% of coarse above-ground stem litter, all other litter, and all above-ground herbaceous plant parts (Hao et al., 1990). Charcoal production was ignored. (iii) The remaining litter was apportioned to coarse and fine litter above- and below-ground. (iv) Soil disturbance in the year of deforestation was

assumed to cause 30% of the carbon in protected pools to move to the active decomposable pools.

- *Cropland*. (i) Tree regeneration was prevented. (ii) Cultivation caused 30% of the carbon in protected pools to move to the active decomposable pools every year. (iii) Harvesting removed 50% of above-ground vegetation carbon every year. No account was taken of the fate of crop products. The remaining carbon was transferred to litter. (iv) Incorporation of litter was simulated by assuming that 50% of the above-ground structural and metabolic litter pools were transferred to the topsoil structural and metabolic litter pools each year of cultivation (Voroney and Angers, 1995; van Veen and Kuikman, 1990).

References

- Bot, A.J., Nachtergaele, F.O., Young, A., 2000. Land Resource Potential and Constraints at Regional And Country Levels. FAO, Rome, p. 122.
- Comins, H.N., McMurtrie, R.E., 1993. Long-term response of nutrient-limited forests to CO₂ enrichment-equilibrium behavior of plant-soil models. *Ecological Applications* 3, 666–681.
- Cox, P.M., Betts, R.A., Jones, C.D., Spall, S.A., Totterdell, I.J., 2000. Acceleration of global warming due to carbon-cycle feedbacks in a coupled climate model. *Nature* 408, 184–187.
- Cramer, W., Kicklighter, D.W., Bondeau, A., Moore, B., Churkina, C., Nemry, B., Ruimy, A., Schloss, A.L., 1999. Comparing global models of terrestrial net primary productivity (NPP): overview and key results. *Global Change Biology* 5, 1–15.
- DeFries, R.S., Field, C.B., Fung, I., Collatz, G.J., Bounoua, L., 1999. Combining satellite data and biogeochemical models to estimate global effects of human-induced land cover change on carbon emissions and primary productivity. *Global Biogeochemical Cycles* 13, 803–815.
- Dewar, R.C., Medlyn, B.E., McMurtrie, R.E., 1999. Acclimation of the respiration photosynthesis ratio to temperature: insights from a model. *Global Change Biology* 5, 615–622.
- Farquhar, G.D., von Caemmerer, S., 1982. Modelling of photosynthetic response to environmental conditions. In: Lange, O.L., Nobel, P., Osmond, C.B., Ziegler, H. (Eds.), *Physiological Plant Ecology II. Water Relations and Carbon Assimilation*, Vol. 12B. Springer, Berlin, pp. 549–587.
- Friend, A.D., 1995. Pgen—an integrated model of leaf photosynthesis, transpiration, and conductance. *Ecological Modelling* 77, 233–255.
- Friend, A.D., White, A., 2000. Evaluation and analysis of a dynamic terrestrial ecosystem model under preindustrial conditions at the global scale. *Global Biogeochemical Cycles* 14, 1173–1190.
- Friend, A.D., Stevens, A.K., Knox, R.G., Cannell, M.G.R., 1997. A process-based, terrestrial biosphere model of ecosystem dynamics (Hybrid v3.0). *Ecological Modelling* 95, 249–287.
- Gifford, R.M., 1995. Whole plant respiration and photosynthesis of wheat under increased CO₂ concentration and temperature: long-term vs short-term distinctions for modelling. *Global Change Biology* 1, 385–396.
- Hao, W.M., Liu, M.-H., Crutzen, P.J., 1990. Estimates of annual and regional releases of CO₂ and other trace gases to the atmosphere from fires in the tropics, based on the FAO statistics for the period 1975–80. In: Goldammer, J.G. (Ed.), *Fire in the Tropical Biota. Ecosystem Processes and Global Challenges*, Vol. 84. Springer, Berlin, pp. 440–462.
- Houghton, R.A., 1991. Releases of Carbon to the atmosphere from degradation of forests in Tropical Asia. *Canadian Journal of Forest Research—Revue Canadienne De Recherche Forestiere* 21, 132–142.
- Houghton, R.A., 1995. Land-use change and the carbon-cycle. *Global Change Biology* 1, 275–287.
- IPCC, 2000. Emissions Scenarios. A Special Report of Working Group II of the Intergovernmental Panel on Climate Change. In: Cambridge University Press, Cambridge 612pp.
- IPCC, 2001. Climate Change 2001: the scientific basis. Summary for Policymakers, IPCC, Geneva, p. 881.
- Jarvis, P.G., 1976. The interpretation of the variations in leaf water potential and stomatal conductance found in canopies in the field. *Philosophical Transactions of the Royal Society of London (B)* 273, 593–610.
- Jarvis, P.G., 1998. European Forests and Global Change: the likely Impacts of Rising CO₂ and Temperature, Cambridge University Press, Cambridge, p. 380.
- McGuire, A.D., Sitch, S., Clein, J.S., Dargaville, R., Esser, G., Foley, J., Heimann, M., Joos, F., Kaplan, J., Kicklighter, D.W., Meier, R.A., Melillo, J.M., Moore, B., Prentice, I.C., Ramankutty, N., Reichenau, T., Schloss, A., Tian, H., Williams, L.J., Wittenberg, U., 2001. Carbon balance of the terrestrial biosphere in the twentieth century: analyses of CO₂, climate and land use effects with four process-based ecosystem models. *Global Biogeochemical Cycles* 15, 183–206.
- Monteith, J.L., Unsworth, M.H., 1990. *Principles of Environmental Physics*. Edward Arnold, London, p. 291.
- Olson, J.S., Watts, J.A., Allison, L.J., 1983. Carbon in Live Vegetation of Major World Ecosystems. Oak Ridge National Laboratory, Oak Ridge, Tennessee, p. 154.
- Ramankutty, N., Foley, J.A., 1999. Estimating historical changes in global land cover: croplands from 1700 to 1992. *Global Biogeochemical Cycles* 13, 997–1027.
- Ramankutty, N., Foley, J.A., Norman, J., McSweeney, K., 2002. The global distribution of cultivable lands: current patterns and sensitivity to possible climate change. *Global Ecology and Biogeography* 11, 377–392.
- Ryan, M.G., 1991. Effects of climate change on plant respiration. *Ecological Applications* 1, 157–167.
- Sellers, P.J., Berry, J.A., Collatz, G.J., Field, C.B., Hall, F.G., 1992. Canopy reflectance, photosynthesis, and transpiration 0.3. A reanalysis using improved leaf models and a new canopy integration scheme. *Remote Sensing of Environment* 42, 187–3216.
- Stewart, J.B., 1988. Modelling surface conductance of pine forest. *Agricultural and Forest Meteorology* 43, 19–335.
- Thornley, J.H.M., Cannell, M.G.R., 2000. Modelling the components of respiration: representation and realism. *Annals of Botany* 85, 55–67.
- van Veen, J.A., Kuikman, P.J., 1990. Soil structure. *Biogeochemistry* 11, 213–233.
- Voroney, R.P., Angers, D.A., 1995. Analysis of the short-term effects of management on soil organic matter using the Century model. In: Lal, R., Kimble, J., Levine, E., Stewart, B.A. (Eds.), *Soil Management and Greenhouse Effect*. Lewis Publishers, Boca Raton, pp. 113–120.
- Waring, R.H., Landsberg, J.J., Williams, M., 1998. Net primary production of forests: a constant fraction of gross primary production? *Tree Physiology* 18, 129–134.